

Determining the Chirality of Yukawa Couplings via Single Charged Higgs Boson Production in Polarized Photon Collision

HONG-JIAN HE¹, SHINYA KANEMURA², C.-P. YUAN²

¹*Center for Particle Physics, University of Texas at Austin, Texas 78712, USA*

²*Department of Physics and Astronomy, Michigan State University, East Lansing, Michigan 48824, USA*

When the charged Higgs boson is too heavy to be produced in pairs, the predominant production mechanism at Linear Colliders is via the single charged Higgs boson production processes, such as $e^-e^+ \rightarrow b\bar{c}H^+$, $\tau\bar{\nu}H^+$ and $\gamma\gamma \rightarrow b\bar{c}H^+$, $\tau\bar{\nu}H^+$. We show that the yield of a heavy charged Higgs boson at a $\gamma\gamma$ collider is typically one or two orders of magnitude larger than that at an e^-e^+ collider. Furthermore, a polarized $\gamma\gamma$ collider can determine the chirality of the Yukawa couplings of fermions with charged Higgs boson via single charged Higgs boson production, and thus discriminate models of new physics.

PACS numbers: 12.60.-i, 12.15.-y, 11.15.Ex

[March, 2002 and hep-ph/0203090]

I. INTRODUCTION

The detection of a charged Higgs boson unambiguously signals new physics beyond the Standard Model (SM) of particle physics. In most extensions of the SM, the mass (M_{H^\pm}) of a charged Higgs boson (H^\pm) is predicted to be around the weak scale. At hadron colliders, such as the Fermilab Tevatron and the CERN Large Hadron Collider (LHC), a light charged Higgs boson can be produced from the decay of top quark via $t \rightarrow H^+b$, if $M_{H^\pm} > m_t - m_b$, where m_t and m_b are the masses of top and bottom quarks, respectively [1]. Otherwise, it can be produced in pairs via the s -channel $q\bar{q}$ fusion process [2] through the gauge interactions of γ - H^+H^- and Z - H^+H^- . However, the rate of the pair production is generally smaller than that predicted by the single charged Higgs boson production mechanisms as the mass of the charged Higgs boson increases. At hadron colliders, a single charged Higgs boson can be produced via $gb \rightarrow H^\pm t$ [3], $cs, cb \rightarrow H^\pm$ [4, 5], and gg (or $q\bar{q}$) $\rightarrow H^\pm W^\mp$ [6], etc. While the single charged Higgs boson production rate at hadron colliders can be sizable, it is extremely difficult to determine the chirality of the Yukawa couplings of fermions with charged Higgs boson. In this work, we show that it can be readily achieved at a polarized photon collider.

If M_{H^\pm} is smaller than half of the center-of-mass energy (\sqrt{s}) of a Linear Collider (LC), then H^\pm can be copiously produced in pairs via the scattering processes $e^-e^+ \rightarrow H^-H^+$ and $\gamma\gamma \rightarrow H^-H^+$ [7]. The production rate of a H^-H^+ pair is determined by the electroweak gauge interaction of H^\pm and gauge bosons, which depends only on the electric charge and weak-isospin of H^\pm . When $M_{H^\pm} > \sqrt{s}/2$, it is no longer possible to produce the charged Higgs bosons in pairs. In this case, the predominant production mechanism of the charged Higgs boson is via the single charged Higgs boson production processes, such as the loop induced process $e^-e^+ \rightarrow H^\pm W^\mp$ [8], and the tree level processes

$e^-e^+ \rightarrow b\bar{c}H^+$, $\tau\bar{\nu}H^+$ and $\gamma\gamma \rightarrow b\bar{c}H^+$, $\tau\bar{\nu}H^+$. The production rate of the above tree level processes depends on the Yukawa couplings of fermions with H^\pm . This makes it possible to discriminate models of flavor symmetry breaking by measuring the production rate of the single charged Higgs boson at the LC. We find that the yield of a heavy charged Higgs boson at a $\gamma\gamma$ collider is typically one or two orders of magnitude larger than that at an e^-e^+ collider. [In this paper, we assume the center-of-mass energy of a $\gamma\gamma$ collider ($\sqrt{s}_{\gamma\gamma}$) is about 80% of that of an e^-e^+ collider (\sqrt{s}_{ee})].

It is well known that the main motivation for building a high-energy polarized photon collider is to determine the CP property of the neutral Higgs bosons [9]. In this study, we provide another motivation for having a polarized photon collider – to determine the chirality of the Yukawa coupling of fermions with charged Higgs boson via single charged Higgs boson production so as to discriminate models of flavor symmetry breaking.

II. YUKAWA INTERACTIONS IN NEW PHYSICS MODELS

The well-motivated new physics models that contain a charged Higgs boson can be classified into the weakly interacting models (with elementary Higgs scalars) [10] and the strongly interacting models (with composite Higgs scalars) [11]. A typical example of the weakly interacting models is the Minimal Supersymmetric SM (MSSM) [12], and of the strongly interacting models is the dynamical Top-color (TopC) model [13]. In general, the Yukawa coupling of the fermions with H^\pm can be written as

$$\mathcal{L}_Y = \overline{f'} \left(Y_L^{f'f} P_L + Y_R^{f'f} P_R \right) f H^- + \text{h.c.}, \quad (1)$$

where f and f' represent up-type and down-type fermions, respectively, and $P_{L,R}$ are the chirality projection operators $P_{L,R} = (1 \mp \gamma_5)/2$.

We first consider the Yukawa sector of the MSSM, which is similar to that of a Type-II 2HDM. The corresponding tree-level Yukawa couplings of fermions with H^\pm are given by

$$Y_{L(0)}^{f'f} = \frac{\sqrt{2}m_{f'}}{v} V_{ff'} \tan\beta, \quad Y_{R(0)}^{f'f} = \frac{\sqrt{2}m_f}{v} V_{ff'} \cot\beta, \quad (2)$$

where m_f ($m_{f'}$) is the mass of fermion f (f'), $\tan\beta = \langle H_u \rangle / \langle H_d \rangle$ is the ratio of the vacuum expectation values of two Higgs doublets, $v = (\langle H_u \rangle^2 + \langle H_d \rangle^2)^{1/2} \simeq 246$ GeV, and $V_{ff'}$ is the relevant Cabibbo-Kobayashi-Maskawa (CKM) matrix element. The coupling constants $Y_{L(0)}^{f'f}$ and $Y_{R(0)}^{f'f}$ vary as the input parameter $\tan\beta$ changes. For the $\bar{\tau}\nu$ - H^- coupling, $Y_{L(0)}^{\tau\nu}$ increases as $\tan\beta$ grows, and reaches about $0.20 - 0.51$ for $\tan\beta = 20 - 50$, while $Y_{R(0)}^{\tau\nu}$ is zero because of the absence of right-handed Dirac neutrinos in the MSSM. As a typical choice for large $\tan\beta$, we take

$$(Y_{L(0)}^{\tau\nu}, Y_{R(0)}^{\tau\nu}) \simeq (0.3, 0), \quad \text{for } \tan\beta \simeq 30. \quad (3)$$

The tree level \bar{b} - c - H^- coupling contains a CKM suppression factor $V_{cb} \simeq 0.04$, so that $Y_{L(0)}^{bc}$ is around 0.03 for $\tan\beta = 50$ and $Y_{R(0)}^{bc}$ is less than about 2×10^{-4} for $\tan\beta > 2$. However, the SUSY radiative correction can significantly enhance the tree level \bar{b} - c - H^- coupling. It was shown in Ref. [4] that the radiatively generated \bar{b} - c - H^- coupling from the natural stop-scharm ($\tilde{t} - \tilde{c}$) mixing in the SUSY soft-breaking sector can be quite sizable. For instance, in the minimal Type-A1 SUSY models [4], the non-diagonal scalar trilinear A -term for the up-type squarks can induce the Yukawa couplings of b - c - H^\pm , such that for $\tan\beta = 50$, Y_L^{bc} is around 0.05 and Y_R^{bc} is about 0. One important feature of the fermion Yukawa couplings in the MSSM is that for a large $\tan\beta$, $Y_L^{f'f}$ can be at the order 1, but $Y_R^{f'f}$ is about 0. This feature will be relevant to our latter discussion on how to use a polarized photon collider to discriminate models of new physics by testing the chirality structure of the fermion Yukawa couplings.

We now turn to the TopC model [13], which provides an attractive scenario for explaining the large top quark mass from the $\langle \bar{t}t \rangle$ condensation via the strong $SU(3)_{\text{tc}}$ TopC interaction at the TeV scale. The associated strong tilting $U(1)$ force is attractive in the $\langle \bar{t}t \rangle$ channel and repulsive in the $\langle \bar{b}b \rangle$ channel, so that the bottom quark mainly acquires its mass from the TopC instanton contribution [13]. This model predicts three relatively light physical top-pions (π_t^0, π_t^\pm). The Yukawa interactions of these top-pions with the b, t and c (charm) quarks can be written as

$$\begin{aligned} & \frac{m_t \tan\beta'}{v} \left[i K_{UR}^{tt} K_{UL}^{tt*} \bar{t}_L t_R \pi_t^0 + \sqrt{2} K_{UR}^{tt} K_{DL}^{bb*} \bar{b}_L t_R \pi_t^- + \right. \\ & \left. i K_{UR}^{tc} K_{UL}^{tc*} \bar{t}_L c_R \pi_t^0 + \sqrt{2} K_{UR}^{tc} K_{DL}^{bb*} \bar{b}_L c_R \pi_t^- + \text{h.c.} \right], \end{aligned} \quad (4)$$

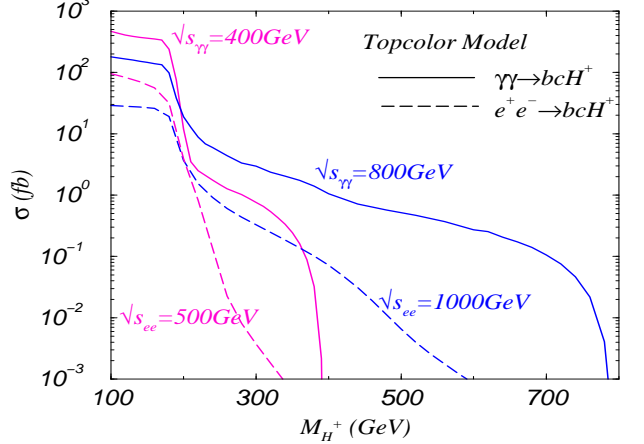


FIG. 1: Cross sections of $\gamma\gamma \rightarrow b\bar{c}H^+$ (solid curves) and $e^+e^- \rightarrow b\bar{c}H^+$ (dashed curves) for the TopC model [cf. Eq. (5)] with unpolarized photon beams at $\sqrt{s}_{\gamma\gamma} = 400$ (800) GeV and $\sqrt{s}_{ee} = 500$ (1000) GeV.

where $\tan\beta' = \sqrt{(v/v_t)^2 - 1}$ and the top-pion decay constant $v_t \simeq O(60 - 100)$ GeV. The rotation matrices $K_{UL,R}$ and $K_{DL,R}$ are needed for diagonalizing the up- and down-quark mass matrices M_U and M_D , i.e., $K_{UL}^\dagger M_U K_{UR} = M_U^{\text{dia}}$ and $K_{DL}^\dagger M_D K_{DR} = M_D^{\text{dia}}$, from which the CKM matrix is defined as $V = K_{UL}^\dagger K_{DL}$. To yield a realistic form of the CKM matrix V (such as the Wolfenstein-parametrization), the TopC model generally predicts $K_{UR}^{tt} \simeq 0.99 - 0.94$, $K_{UR}^{tc} \lesssim 0.11 - 0.33$, and $K_{UL}^{tt} \simeq K_{DL}^{bb} \simeq 1$, which suggests that the t_R - c_R transition can be naturally around 10–30% [5]. Consequently, the Yukawa couplings of fermions with the charged top-pion (pseudoscalar Higgs boson) are $Y_L^{bt} = Y_L^{bc} = 0$, $Y_R^{bt} \simeq (\sqrt{2}m_t/v) \tan\beta'$, and $Y_R^{bc} \simeq Y_R^{bt} K_{UR}^{tc}$. Thus, taking a typical value of $\tan\beta' \simeq 3$ and a conservative input of $K_{UR}^{tc} \simeq 0.1$ for the t_R - c_R mixing, we obtain

$$Y_R^{bt} \simeq 3, \quad \text{and} \quad (Y_L^{bc}, Y_R^{bc}) \simeq (0, 0.3), \quad (5)$$

which will be used as the sample TopC parameters for our numerical analysis.

As noted earlier, the chirality of the Yukawa couplings of b - c - π_t^\pm is purely right-handed, in contrast to the left-handed Yukawa couplings predicted by the MSSM with a large $\tan\beta$ value, as discussed above. This feature makes it possible to discriminate the dynamical TopC model from the MSSM or a Type-II 2HDM by measuring the production rates of single charged Higgs boson at polarized photon colliders.

III. H^\pm PRODUCTION IN PHOTON COLLISION AS A PROBE OF NEW PHYSICS

Using the default parameters of the model as described in the previous section, cf. Eq. (5), we calculate the total cross sections of $\gamma\gamma \rightarrow b\bar{c}H^+$ and $e^+e^- \rightarrow b\bar{c}H^+$

as a function of M_{H^\pm} . The result is shown in Fig. 1, where we have taken the center-of-mass energy of the $\gamma\gamma$ collider to be 0.8 times of that of the e^-e^+ collider for comparison. A few discussions on the feature of the results shown in Fig. 1 are in order. For $M_{H^\pm} < \sqrt{s}/2$, the charged Higgs bosons can be produced in pairs. In this case, the production cross section for $\gamma\gamma \rightarrow b\bar{c}H^+$ (and $e^-e^+ \rightarrow b\bar{c}H^+$) is dominated by the contribution from the H^-H^+ pair production diagrams with the produced H^- decaying into a $b\bar{c}$ pair. Hence, its rate is proportional to the decay branching ratio $Br(H^- \rightarrow b\bar{c})$. (For example, for a 200 GeV (400 GeV) H^\pm , Γ_H is about 7 GeV (143 GeV), and $Br(H^- \rightarrow b\bar{c})$ is 0.15 (0.015).) As shown in the figure, there is a *kink* structure when M_{H^\pm} is around 180 GeV. That is caused by the change in $Br(H^- \rightarrow b\bar{c})$ when the decay channel $H^- \rightarrow b\bar{t}$ becomes available. Furthermore, for $M_{H^\pm} < \sqrt{s}_{\gamma\gamma}/2$, the cross section in $\gamma\gamma$ collision is typically an order of magnitude larger than that in e^-e^+ collision.

It is evident that the cross section of $\gamma\gamma \rightarrow b\bar{c}H^+$ is larger than that of $e^-e^+ \rightarrow b\bar{c}H^+$ in the whole M_{H^\pm} region. For $M_{H^\pm} > \sqrt{s}/2$, where the pair production is not kinematically allowed, the difference between these two cross sections becomes much larger (two or three orders of magnitude) for a larger M_{H^\pm} value. To understand the cause of this difference, we have to examine the Feynman diagrams that contribute to the scattering processes $e^-e^+ \rightarrow b\bar{c}H^+$ and $\gamma\gamma \rightarrow b\bar{c}H^+$. In the former process, all the Feynman diagrams contain an s -channel propagator which is either a virtual photon or a virtual Z boson. Therefore, when M_{H^\pm} increases for a fixed \sqrt{s}_{ee} , the cross section decreases rapidly. On the contrary, in the latter process, when $M_{H^\pm} > \sqrt{s}_{\gamma\gamma}/2$, the dominant contribution arises from the fusion diagram $\gamma\gamma \rightarrow (c\bar{c})(b\bar{b}) \rightarrow b\bar{c}H^+$, whose contribution is enhanced by the two collinear poles (in a t -channel diagram) generated from $\gamma \rightarrow c\bar{c}$ and $\gamma \rightarrow b\bar{b}$ in high energy collisions. Since the collinear enhancement takes the form of $\ln(M_{H^\pm}/m_q)$, with m_q being the bottom or charm quark mass, the cross section of $\gamma\gamma \rightarrow b\bar{c}H^+$ does not vary much as M_{H^\pm} increases until it is close to $\sqrt{s}_{\gamma\gamma}$.

From the above discussions we conclude that a photon-photon collider is superior to an electron-positron collider to detect a heavy charged Higgs boson. Moreover, a polarized photon collider can determine the chirality of the Yukawa couplings of fermions with charged Higgs bosons via single charged Higgs boson production. This point is illustrated as follows. First, let us consider the case that $M_{H^\pm} > \sqrt{s}_{\gamma\gamma}/2$. As noted above, in this case, the production cross section is dominated by the fusion diagram $\gamma\gamma \rightarrow (c\bar{c})(b\bar{b}) \rightarrow b\bar{c}H^+$. In the TopC model, because $Y_L^{bc} = 0$ (and $Y_R^{bc} \neq 0$), it corresponds to $\gamma\gamma \rightarrow (c_R\bar{c}_R)(b_L\bar{b}_L) \rightarrow b_L\bar{c}_R H^+$. On the other hand, in the MSSM with stop-scharm mixing and large $\tan\beta$, $Y_R^{bc} \sim 0$ (and $Y_L^{bc} \neq 0$), it becomes $\gamma\gamma \rightarrow (c_L\bar{c}_R)(b_R\bar{b}_L) \rightarrow b_R\bar{c}_L H^+$. Therefore, we expect that if both photon beams are right-handedly polarized (i.e. $\gamma_R\gamma_R$), then a TopC charged Higgs boson (top-pion)

can be copiously produced, while a MSSM charged Higgs boson (with a large $\tan\beta$) is highly suppressed. To detect a MSSM charged Higgs boson, both photon beams have to be left-handedly polarized (i.e. $\gamma_L\gamma_L$). This is supported by an exact calculation whose results are shown in Fig. 2(a) for the TopC model. (A similar feature also holds for the MSSM Type-A1 models [4] after interchanging the label of RR and LL in Fig. 2(a).)

The feature of the polarized photon cross sections for $M_{H^\pm} < \sqrt{s}/2$ can be understood from examining the production process $\gamma\gamma \rightarrow H^+H^-$. The helicity amplitudes for the H^+H^- pair production in polarized photon collisions are calculated as

$$M(\gamma_{\lambda_1}\gamma_{\lambda_2} \rightarrow H^+H^-) = 2e^2\lambda_1\lambda_2 \left(\frac{1-\xi^2}{1-\xi^2\cos^2\Theta} \right) + e^2(1-\lambda_1\lambda_2), \quad (6)$$

where the degree of polarization of the initial state photons, λ_1 and λ_2 , can take the value of either -1 or $+1$, corresponding to a left-handedly (L) or right-handedly (R) polarized photon beam, respectively; Θ is the scattering angle of H^+ in the center-of-mass frame; and $\xi = \sqrt{1-4M_{H^\pm}^2/s_{\gamma\gamma}}$. In the massless limit, i.e. when $M_{H^\pm} \rightarrow 0$, the above result reduces to $M(\gamma_{\lambda_1}\gamma_{\lambda_2} \rightarrow H^+H^-) \simeq e^2(1-\lambda_1\lambda_2)$. Denote $\sigma_{\lambda_1\lambda_2}^{\text{pair}}$ as the cross section of $\gamma_{\lambda_1}\gamma_{\lambda_2} \rightarrow H^+H^-$. We find that $\sigma_{LR}^{\text{pair}} = \sigma_{RL}^{\text{pair}}$, and they dominate the total cross section when $M_{H^\pm}^2 \ll s$, while $\sigma_{LL}^{\text{pair}}$ and $\sigma_{RR}^{\text{pair}}$ are equal and approach to zero as $M_{H^\pm} \rightarrow 0$. Since for $M_{H^\pm} < \sqrt{s}_{\gamma\gamma}/2$ the bulk part of the cross section of $\gamma\gamma \rightarrow b\bar{c}H^+$ comes from $\sigma(\gamma\gamma \rightarrow H^+H^-) \times Br(H^- \rightarrow b\bar{c})$, the LL and RR cross sections are smaller than the LR ($= RL$) cross sections as M_{H^\pm} decreases, cf. Fig. 2.

It is important to point out that the complete set of Feynman diagrams has to be included to calculate $\sigma(\gamma\gamma \rightarrow b\bar{c}H^+)$ even when $M_{H^\pm} < \sqrt{s}_{\gamma\gamma}/2$ because of the requirement of gauge invariance. To study the effect of the additional Feynman diagrams, other than those contributing to the H^+H^- pair production from $\gamma\gamma \rightarrow H^+H^- (\rightarrow b\bar{c})$, one can examine the *single* charged Higgs boson rate in this regime with the requirement that the invariant mass of $b\bar{c}$, denoted as $M_{b\bar{c}}$, satisfies the following condition:

$$\begin{aligned} |M_{b\bar{c}} - M_{H^\pm}| &> \Delta M_{b\bar{c}}, \quad \text{with} \\ \Delta M_{b\bar{c}} &= \min \left[25 \text{ GeV}, \max \left[1.18 M_{cb} \frac{2\delta m}{m}, \Gamma_H \right] \right], \\ \frac{\delta m}{m} &= \frac{0.5}{\sqrt{M_{b\bar{c}}/2}}, \end{aligned} \quad (7)$$

where $\frac{\delta m}{m}$ denotes the mass resolution of the detector for observing the final state b and \bar{c} jets originated from the

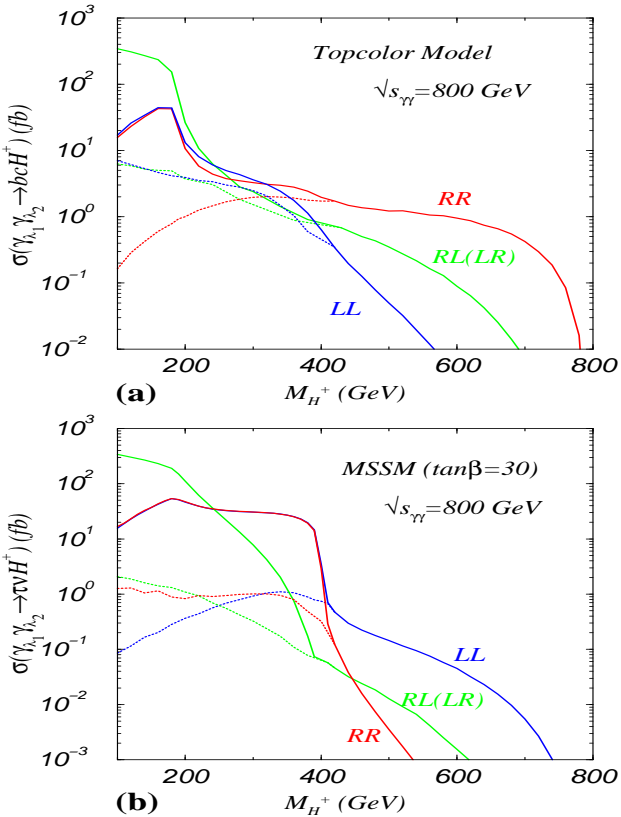


FIG. 2: (a): Cross sections of $\gamma_{\lambda_1}\gamma_{\lambda_2} \rightarrow b\bar{c}H^+$ at $\sqrt{s_{\gamma\gamma}} = 800$ GeV in polarized photon collisions for the TopC model [cf. Eq. (5)]. Solid curves are the results without any kinematical cut, and Dashed curves are the results with the kinematical cuts specified in the text [cf. Eq. (7)]. (b): Cross sections of $\gamma_{\lambda_1}\gamma_{\lambda_2} \rightarrow \tau\nu H^+$ at $\sqrt{s_{\gamma\gamma}} = 800$ GeV in polarized photon collisions for the MSSM [cf. Eq. (3)].

decay of H^- . For example, in Fig. 2(a) the set of dashed-lines are the polarized cross sections after imposing the above kinematical cut. With this cut, the total rate reduces by about one order of magnitude for $M_{H^\pm} < \sqrt{s_{\gamma\gamma}}/2$. (Needless to say that this cut can hardly change the event rate when $M_{H^\pm} > \sqrt{s_{\gamma\gamma}}/2$.)

The effect of this kinematic cut on the RR and LL rates are significantly different in the low M_{H^\pm} region. It implies that the H^+H^- pair production diagrams cannot be the whole production mechanism, otherwise, we would expect the rates of RR and LL be always equal due to the parity invariance of the QED theory. (Again, a similar feature also holds for the MSSM Type-A1 models [4] after interchanging the labels of LL and RR .) In Fig. 2(b), we show the results for $\gamma_{\lambda_1}\gamma_{\lambda_2} \rightarrow \tau\nu H^+$ in the MSSM with $\tan\beta = 30$.

IV. CONCLUSIONS

The single charged Higgs boson can be produced at polarized photon colliders via the scattering processes $\gamma\gamma \rightarrow b\bar{c}H^+$ and $\gamma\gamma \rightarrow \tau\nu H^+$. We have shown that the production rate of H^\pm in the $\gamma\gamma$ collision is much larger than that in the e^+e^- collision, cf. Fig. 1. For $M_{H^\pm} > \sqrt{s}/2$, the e^+e^- rate is smaller by at least one or two orders of magnitude than the $\gamma\gamma$ rate. This is because in high energy collisions there are two collinear poles ($\gamma\gamma \rightarrow (c\bar{c})(b\bar{b}) \rightarrow b\bar{c}H^+$) in $\gamma\gamma \rightarrow b\bar{c}H^+$, while the e^+e^- processes contain only s -channel diagrams and cannot generate any collinear enhancement factor to the single charged Higgs boson production rate. Furthermore, we find that it is possible to measure the Yukawa couplings Y_L and Y_R , separately, at photon-photon colliders by properly choosing the polarization states of the incoming photon beams. This unique feature of the photon colliders can be used to discriminate models of flavor symmetry breaking. Hence, we conclude that a polarized photon-photon collider is not only useful for determining the CP property of a neutral Higgs boson, but also useful for detecting a heavy charged Higgs boson and determining the chirality of the Yukawa couplings of fermions with charged Higgs boson.

Acknowledgments We thank Gordon L. Kane for valuable discussions on the SUSY flavor mixing. SK would like to thank Stefano Moretti for useful discussions and for comparing part of our results with his calculation. This work was supported in part by the NSF grant PHY-9802564 and DOE grant DEFG0393ER40757.

[1] B. Abbott *et al.* [DØ Collaboration], *Phys. Rev. Lett.* **82** (1999) 4975.
[2] A.A. Barrientos Bendezu and B.A. Kniehl, *Nucl. Phys. B* **568** (2000) 305; O. Brein and W. Hollik, *Euro. Phys. J. C* **13** (2000) 175.
[3] J. Gunion, G. Ladinsky, C.-P. Yuan, *et al.*, Snowmass Summer Study 1990:0059-81 (QCD161:D15:1990); V. Barger, R.J.N. Phillip and D.P. Roy, *Phys. Lett. B* **324** (1994) 236; A. Belyaev, D. Garcia, J. Guasch, J. Solà, hep-ph/0203031.
[4] J. L. Diaz-Cruz, H.-J. He, C.-P. Yuan, *Phys. Lett. B* (in press), hep-ph/0103178.
[5] H.-J. He and C.-P. Yuan, *Phys. Rev. Lett.* **83** (1999) 28.
[6] O. Brein, W. Hollik and S. Kanemura, *Phys. Rev. D* **63** (2001) 095001, and references therein.
[7] S. Komamiya, *Phys. Rev. D* **38** (1988) 2158.
[8] S. Kanemura, *Euro. Phys. J. C* **17** (2000) 473, S. Kanemura, S. Moretti and K. Odagiri, *JHEP* 0102 (2001) 011, and references therein.
[9] E. Asakawa, S.Y. Choi, K. Hagiwara and J.-S. Lee, *Phys. Rev. D* **62** (2000) 115005, and references therein.
[10] See, for instance, reviews in “Perspectives on Supersymmetry”, ed. G. L. Kane, World Scientific Pub, 1998.
[11] See, for instance, R. S. Chivukula, hep-ph/0011264.
[12] See, for instance, H. E. Haber, *Nucl. Phys. Proc. Suppl.* **101** (2001) 217.
[13] C. T. Hill, *Phys. Lett. B* **345**, 483 (1995); *Phys. Lett. B* **266**, 419 (1991).